Journal of Geophysical Research: Oceans

RESEARCH ARTICLE
10.1002/2017JC013472

Mapping Dependence Between Extreme Rainfall and Storm Surge

Wenyan Wu[1,2], Kathleen McInnes[3], Julian O'Grady[3], Ron Hoeke[3], Michael Leonard[2], and Seth Westra[2]

[1]Department of Infrastructure, University of Melbourne, Melbourne, Vic, Australia, [2]School of Civil, Environmental and Mining Engineering, University of Adelaide, Adelaide, SA, Australia, [3]Commonwealth Scientific and Industrial Research Organisation, Marine and Atmospheric Research, Aspendale, Vic, Australia

Key Points:
- The Regional Ocean Modeling System is used to produce dependence maps of extreme storm surge and rainfall along the Australian coastline
- Different synoptic patterns are responsible for rain-only, surge-only, and coincident extremes
- Care is required when estimating dependence using reanalysis data at locations where there are multiple processes driving extremes

Supporting Information:
- Supporting Information S1

Correspondence to:
W. Wu,
wenyan.wu@unimelb.edu.au

Citation:
Wu, W., McInnes, K., O'Grady, J., Hoeke, R., Leonard, M., & Westra, S. (2018). Mapping dependence between extreme rainfall and storm surge. *Journal of Geophysical Research: Oceans*, *123*, 2461–2474. https://doi.org/10.1002/2017JC013472

Received 19 SEP 2017
Accepted 13 MAR 2018
Accepted article online 23 MAR 2018
Published online 6 APR 2018

Abstract Dependence between extreme storm surge and rainfall can have significant implications for flood risk in coastal and estuarine regions. To supplement limited observational records, we use reanalysis surge data from a hydrodynamic model as the basis for dependence mapping, providing information at a resolution of approximately 30 km along the Australian coastline. We evaluated this approach by comparing the dependence estimates from modeled surge to that calculated using historical surge records from 79 tide gauges around Australia. The results show reasonable agreement between the two sets of dependence values, with the exception of lower seasonal variation in the modeled dependence values compared to the observed data, especially at locations where there are multiple processes driving extreme storm surge. This is due to the combined impact of local bathymetry as well as the resolution of the hydrodynamic model and its meteorological inputs. Meteorological drivers were also investigated for different combinations of extreme rainfall and surge—namely rain-only, surge-only, and coincident extremes—finding that different synoptic patterns are responsible for each combination. The ability to supplement observational records with high-resolution modeled surge data enables a much more precise quantification of dependence along the coastline, strengthening the physical basis for assessments of flood risk in coastal regions.

Plain Language Summary Flood events in coastal and estuarine regions can be caused by a combination of extreme ocean levels due to factors such as high tides and storm surges, and extreme rainfall occurring on the upstream catchments. This study looked at a measure of the likelihood that storm surges and extreme rainfall events occur at the same time (the 'dependence'), and the synoptic weather features such as tropical cyclones that cause these events to co-occur. The analysis examined historical rainfall events from 5,300 rain gauges located throughout Australia, and combined this with information on historical surge events from 79 separate tide gauges distributed along the Australian coastline. The instrumental data was supplemented by outputs from a mathematical model of storm surge, which enabled an assessment of dependence at high resolution and at locations where observational data was sparse. The results indicated that the dependence can change significantly along the Australian coastline, and depended on local weather patterns. The improved understanding of the interaction between storm surge and extreme rainfall events strengthens the physical basis for assessment of flood risk in Australia's coastal and estuarine regions.

1. Introduction

Floods in coastal and estuarine regions can be caused by multiple mechanisms, including elevated sea levels caused by meteorological and nonmeteorological drivers, large runoff generated by extreme rainfall, or both processes occurring at the same time. Such multimechanism events are referred to as "compound events" (Intergovernmental Panel on Climate Change, 2012; Leonard et al., 2014), and are due to extreme rainfall and storm surge often being driven by a common meteorological forcing (McInnes et al., 2002; McInnes & Hubbert, 2001; Wahl et al., 2015). This can lead to significantly increased flood risk for countries like Australia, where over 85% of its population lives within 50 kilometers of the coast (Australian Bureau of Statistics, 2004). Flood management approaches that neglect the potential impact of interacting flood

drivers can lead to misspecification of flood risk, and result in costly or ineffective mitigation approaches (e.g., under-designed flood-protection infrastructure, inappropriate land use controls, etc.). Therefore, a compound event framework that takes into account the dependence of storm surge and extreme rainfall is required to assess flood risk in coastal and estuarine regions (Svensson & Jones, 2002, 2004).

The coincidence of extreme flood drivers in coastal and estuarine regions was documented in Australia as early as the 1910s (Hunt, 1914) and appeared in scientific journals in the 1970s when Hopley (1974) described extreme surge and rainfall caused by tropical cyclone Althea. Since these early studies, there have been numerous attempts to estimate flood levels in estuarine regions as a result of the joint impact of different flood drivers. One general approach is the use of a hydraulic model with continuous time series of boundary inputs representing fluvial and tidal processes, which can be used to develop a statistical distribution of water levels at the location(s) of interest (Acreman, 1994; Lambert & Kuczera, 1996). This approach does not need to explicitly parameterize the dependence between the two processes because dependence is captured in observed boundary inputs. However, long time series are required to adequately sample the joint distribution, especially the extremes, so that continuous simulation is often computationally prohibitive.

An alternative approach is to quantify the strength of dependence between extreme drivers so that they may be used with event-based methods of design. Flood applications have featured prominently in the development of statistical methods for joint extremes (Hashino, 1985; Loganathan et al., 1987). Specifically, the tail dependence measure (Coles et al., 1999; Ledford & Tawn, 1997) can be used to measure the asymptotic dependence between processes such as storm surge, river flow, and rainfall (Hawkes, 2008; Svensson & Jones, 2002, 2004). A bivariate extreme value model was used to quantify the dependence between extreme storm surge and rainfall above appropriately high thresholds along the Australian coastline (Zheng et al., 2013). Similar to bivariate extreme value distributions, copula-based distributions have been applied due to their considerable flexibility in representing the dependence of extremes (Lian et al., 2013), including hierarchical methods that allow copulas to span multiple sites (Bevacqua et al., 2017).

Despite advances in the variety of models and methods used for estimating dependence, developing reliable estimates from the historical record can be challenging due to limited data coverage, data quality, and record length (Muis et al., 2016; Van den Hurk et al., 2015). For example, in the study by Zheng et al. (2013) the dependence was estimated for 49 tide gauge locations around Australia, which only accounts for a very small portion of the Australian coastline. Not only are the gauges sparsely located, but even for two adjacent locations the dependence estimates may be very different (Zheng et al., 2013). This is because the dependence between oceanic and fluvial processes is not only determined by large-scale meteorological effects, but also by local bathymetry and estuary properties that affect storm surge (Resio & Westerink, 2008; Zheng et al., 2013), and by local catchment conditions that affect the rainfall-runoff process (Pathiraja et al., 2012). The potential for local variation in dependence indicates a need to estimate dependence at a much finer resolution. In addition, dependence calculated using historical data may not be appropriate when assessing future flood risk under changing meteorological conditions due to shifts in the climate pattern. Consequently, it is important to understand the meteorological processes that drive different extreme conditions for assessment of flood risk under both historical and changing climates (Wahl et al., 2015). This understanding can also support flood forecasting and flood warning systems, which rely on the modeling of meteorological processes (Casagrande et al., 2017).

To improve the understanding of dependence in flood-producing extremes, we propose to use hydrodynamically modeled storm surge to estimate dependence between extreme surge and rainfall. We examine the suitability of this approach along the Australian coastline by comparing modeled dependence values to estimates from gauged observations. We also analyze the meteorological drivers of different extreme conditions along the Australian coast by examining synoptic patterns related to single-variable and coincident extreme conditions, which provides understanding on whether the meteorological drivers of joint events can be distinguished from situations where only a single variable is extreme. This analysis is further strengthened by investigating the role of seasonal and spatial variability in the dependence and its link to different meteorological processes.

This paper is organized as follows. First, the data used in this study, including both observed data and reanalysis data, are presented in section 2. The methods used to estimate the dependence between

extreme storm surge and rainfall, and the meteorological drivers of different extremes are introduced in section 3. In section 4, dependence values between extreme surge and rainfall estimated using reanalysis and observed surge data are compared. Synoptic patterns related to single-variable and coincident extreme conditions are also investigated. In addition, the seasonal and spatial variability in the dependence along the Australian coastline is discussed. Finally, the summary and conclusions are presented in section 5.

2. Data

2.1. Observed Daily Rainfall

Daily rainfall records from 17,773 stations across Australia were obtained from the Australian Bureau of Meteorology. Stations with very short records (i.e., $<$10 years) or a large number of missing or unreliable data (i.e., $>$10%) were removed, resulting in a final data set of 5,300 stations. The spatial coverage and record length of these rainfall stations are presented in Figure 1. There is good coverage of daily rainfall records along the east, south-east, and south-west coast of Australia near the state capitals. Coverage is more spread out along the north and north-west coast of Australia.

2.2. Observed Storm Surge

Sea level data were obtained for 79 tide gauges around Australia from the Bureau of Meteorology based on two separate data sets. The first data set includes high quality data from 15 tide gauges monitored as part of the Australian Baseline Sea Level Monitoring Project (ABSLMP) (http://www.bom.gov.au/oceanography/projects/abslmp/data/index.shtml). This data set spans from early 1990s to 2015, except for Port Stanvac, where the record ends in 2010. The second data set consists of sea level data from 64 tide gauges maintained by Australian port authorities. The record has various lengths ranging from less than 10 years (e.g., Lakes Entrance in Victoria) to over 100 years (e.g., Fremantle in Western Australia).

The ABSLMP data were aggregated based on 6 min sea level data, whereas the Australian port authorities' data set consists of a combination of hourly point readings from tide gauge records and a range of other sampling intervals, such as 2, 5, or 15 min (Westra, 2012). The sea level data represents the combined water levels resulting from astronomical tides, storm surge due to low pressure systems and other factors that have an impact on ocean water levels including higher frequency oscillations of sea levels, such as infragravity waves or meteotsunamis. The astronomical tide data were extracted from the sea level data using harmonic analysis as described in Pugh (1987) and the Australian Tides Manual (Permanent Committee on Tides and Mean Sea Level, 2007) using 112 tidal constituents (Westra, 2012). In the tidal analysis, a trend term was also used to represent mean sea level change. The storm surge data are nontidal residuals, which are the difference between the sea level values and the tide values. The locations of the tide gauges from the two data sets are shown in Figure 2, and a summary of the data is provided in supporting information Table S1. Only the storm surge data were used in this study, with the dependence analysis being based on the daily maximum surge data.

In order to assess the availability of rainfall data to estimate the dependence between rainfall and storm surge across the Australian coastline, the number of daily rain stations within a 100 km radius of each of the 79 tide gauges is plotted in Figure 3a. In a previous study using observed data only, a 30 km radius was used (Zheng et al., 2013). The value of the radius has been increased to 100 km in this study to account for remote locations where there are no rain gauges within a 30 km radius of a coastal location. It can be seen that overall, the south and east coasts of Australia are well covered; especially along the south-west and south-east coast of Australia, most tide gauges have more than 50 daily rain stations within a 100 km radius (i.e., the black dots in Figure 3a). There is less rainfall information available along the north and northwest coast of Australia. Within this region, only Darwin (i.e., the red dot in north of Australia near Timor Sea in Figure 3a) has between 11 and 50 daily rain stations within 100 km of its radius. In contrast, even with a 100 km radius there is no rainfall station near Nardana Patches (near the Arafura Sea) on the northeast tip of Australia. Although the radius used in the Zheng et al. (2013) study is different from the radius used here, the dependence results

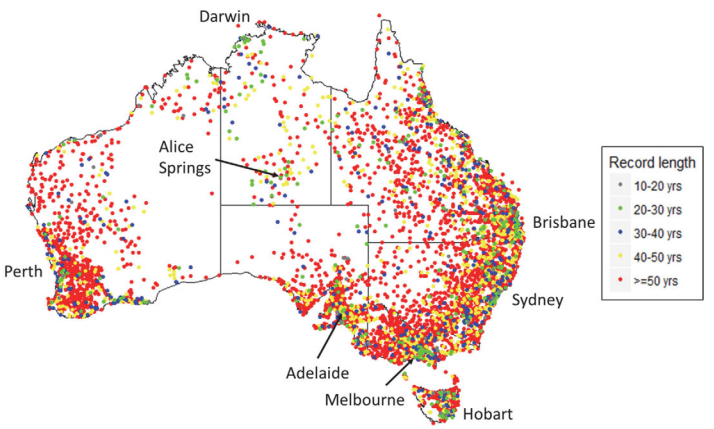

Figure 1. Locations of 5,300 rainfall gauges with color indicating record length.

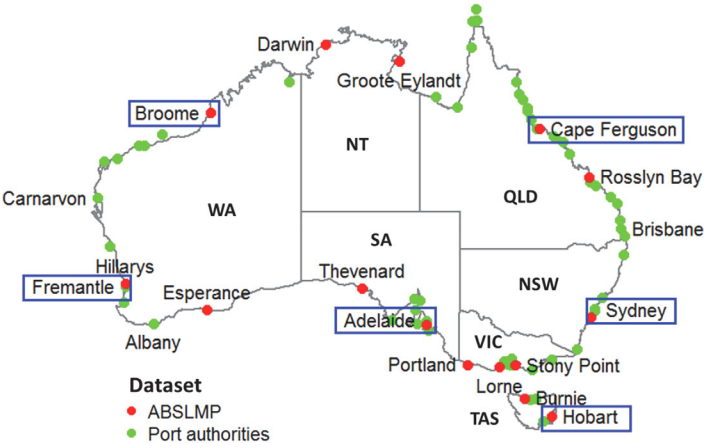

Figure 2. Locations of the 79 tide gauges: red dots represent the 15 tide gauges monitored as part of the Australian Baseline Sea Level Monitoring Project (ABSLMP) and green dots represent the 64 tide gauges maintained by Australian port authorities. Locations in blue boxes are investigated in detail below. (WA = Western Australia, NT = North Territory, SA = South Australia, QLD = Queensland, NSW = New South Wales, VIC = Victoria, TAS = Tasmania.)

are similar, which indicates the choice of the radius does not have a significant impact on the outcomes of the dependence analysis.

2.3. ROMS Modeled Surge Data

Modeled storm surge data around Australia were generated using the Rutgers version of the Regional Ocean Modeling System (ROMS) (Shchepetkin & McWilliams, 2005). The model, described by Colberg and McInnes (2012), was extended to cover the entire Australian coastline at 5 km resolution. For this study, the model was configured to run in barotropic mode with meteorological forcing (i.e., surge-only forcing with no tidal component), which was obtained from the US National Centers for Environmental Prediction Climate Forecast System Reanalyses (CFSR) (Saha et al., 2010). Reanalyses are reconstructions of meteorological variables in the past, produced by running a weather prediction model that is constrained by observations. Therefore, the modeled surge are "true" surge data, rather than nontidal residuals. The CFSR data set provides meteorological variables, including pressure and wind, across the globe at an hourly time step and approximately 38 km spatial resolution. ROMS was validated using high quality marine data from the 15 tide gauges monitored as part of the ABSLMP between 1993 and 2012. More details of the ROMS implementation can be found in Colberg and McInnes (2012).

Output from the ROMS simulation forced by CFSR data was extracted at an hourly temporal resolution for 7,118 locations along the Australian coast for the period between 1 January 1980 and 7 May 2013. In order to reduce the computational time of subsequent statistical analyses, the 7,118 locations were subsampled to 551 locations along the Australian coast at about 30 km intervals. Again, the daily maximum surge data were used in the dependence analysis. The coverage of daily rain stations within a 100 km radius of the 551 ROMS locations is plotted in Figure 3b.

2.4. Synoptic Data

The mean sea level pressure fields required for the synoptic classification of weather events were obtained from reanalyses developed by the US National Centers for Environmental Prediction (NCEP) (Kalnay et al., 1996). The pressure fields are available on a 2.5 × 2.5° global grid every 6 h from 1958 onward. The NCEP data rather than the CFSR data were used in this instance because of its longer temporal availability.

The lower temporal resolution of the NCEP data does not affect the synoptic typing since only a single map from each rain, surge or coincident event day is used in the synoptic typing procedure (we used the 00 UTC pattern). Since the aim of synoptic typing is to achieve a small but representative number of illustrative weather patterns, the low spatial resolution in NCEP is not considered to be disadvantageous since the

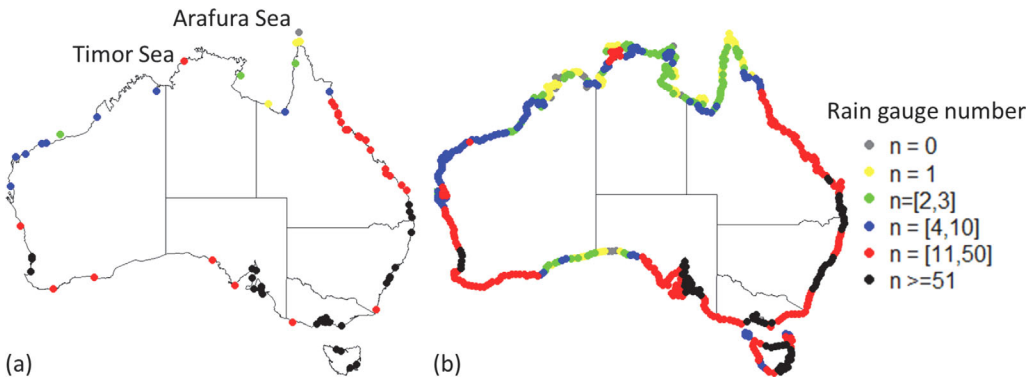

Figure 3. (a) Availability of rain stations within 100 km radius of the 79 tide gauges and (b) the 551 ROMS modeled locations around Australia.

typing procedure involves tuning correlation coefficients to achieve the smallest number of representative patterns. Higher spatial resolution in the analyses would require a lower correlation threshold to reduce the number of distinct maps identified.

3. Methods

The methods used to characterize dependence between rainfall and storm surge (Zheng et al., 2013) are described in this section followed by the method used for the synoptic typing of extreme events.

3.1. The Bivariate Logistic Threshold Excess Model

A method to assess the dependence of two asymptotically dependent variables is the bivariate logistic threshold excess model (Coles, 2001), which has previously been employed in a dependence analysis using observed data (Zheng et al., 2013). The model is described by (Coles, 2001):

$$G(u,v)=\exp\left[-\left(\tilde{u}^{-1/\alpha}+\tilde{v}^{-1/\alpha}\right)^{\alpha}\right] \tag{1}$$

where u and v are realizations of two random variables (e.g., u = rainfall and v = storm surge); G is the bivariate distribution function; $\tilde{u}$ and $\tilde{v}$ are the Fréchet-transformed values of u and v; and α is the dependence parameter.

This well-known model for representing bivariate extreme processes has been shown to be suitable for modeling the dependence between rainfall and storm surge along the Australian coast (Zheng et al., 2013). It has a simple structure, with only one parameter α describing the dependence between two random variables. A value of $\alpha=0$ represents complete dependence, and indicates that if one variable is extreme, the other variable is also extreme. In contrast, $\alpha=1$ represents complete independence, indicating that an extreme value of one variable does not provide information on the value of the other variable. The dependence has a significant impact on the occurrence of coincident extreme events. For example, an α value of 0.95 represents a sevenfold increase of cooccurring extreme events compared to the complete independence case of $\alpha=1$ (Zheng et al., 2013). The censored threshold likelihood method can be used to estimate the value of α (Tawn, 1988). Following Zheng et al. (2013), the threshold value of the 99th percentile was used for analyzing both the rainfall and storm surge data in this study.

3.2. Synoptic Typing

Meteorological drivers of rain-only, surge-only, and coincident extreme events were investigated by synoptically typing mean sea level pressure (MSLP) information at times when these extremes occurred (Yarnal, 1993). The method used is a correlation-based, gridded map-typing technique, in which MSLP maps for the selected dates are grouped based on the Pearson product-moment correlation (r_{xy}). The correlations establish the degree of similarity of spatial structures (i.e., highs and lows in similar positions) between mapped pairs rather than on the magnitude of the highs and lows.

For days on which the rainfall, storm surge, or their combination exceeded the selected 99th percentile threshold at a selected location, MSLP maps at 00 UTC from the NCEP (Kalnay et al., 1996) reanalyses were extracted and normalized via $Z_i=(z_i-\bar{z})/s$, where Z_i is the normalized value at grid point i, z_i is the observed value at grid point i, and $\bar{z}$ and s are the mean and standard deviation of N grid points. The effect of this normalization is to eliminate the seasonal impact on pressure pattern intensity, thus permitting direct interseasonal map comparisons.

Once normalized, each daily map pattern in each extreme event category is compared with all other maps in the same category using the Pearson product-moment correlation (r_{xy}):

$$r_{xy}=\frac{\sum_{i=1}^{N}\left[(x_i-\bar{x})(y_i-\bar{y})\right]}{\sqrt{\sum_{i=1}^{N}(x_i-\bar{x})^2\sum_{i=1}^{N}(y_i-\bar{y})^2}} \tag{2}$$

where x_i and y_i represent the normalized variable at each of the N grid points of the two maps being compared, and $\bar{x}$ and $\bar{y}$ represent the means across the N-point grids. Pairs of MSLP maps are considered similar if $r_{xy} \geq r_t$, where r_t is the correlation threshold. Yarnal (1993) discussed the numerous sources of subjectivity in choosing a correlation threshold. An acceptable balance between the number of patterns produced and

the number of days that were not classified was achieved through experimentation, yielding a value of 0.8 for the rain-only and surge-only events and a value of 0.6 for the coincident events. The different thresholds were used because there are many more dates for extreme rain-only and surge-only events compared to coincident events, and the different thresholds ensured discrimination of sufficiently different map types (see section 4.2 for number of events). A 9 × 9 grid was introduced for estimating pattern similarity of the MSLP maps. Correlations for each row and column of the 9 × 9 grid were calculated to ensure pattern similarity in all areas of the grid covering the maps.

Once all days have been compared with all other days in the data set, the map for which the largest number of other maps met the correlation threshold criteria is designated "key day" 1 and is considered representative of the first map type. This "key day" map and all similar maps based on the r_{xy} threshold being achieved are then removed from the analysis. All days deemed to be similar to each of those days are also removed. The analysis is then repeated with the reduced data set to find "key day" 2, and the process repeats until all days are classified into groups of two days or more. Once the "key days" are established, a second pass over the entire data set is made. This is necessary because it is possible for a given map to be significantly correlated with more than one other map. In this step, each map pattern is assigned to the map pattern represented by the "key day" for which it produces the highest correlation. A second pass was also made over the unclassified days so that the days that had a relatively high correlation value could be classified into the most appropriate synoptic type. A lower correlation threshold of 0.5 was chosen for this step. Finally, the remaining days are considered unclassified.

4. Results and Discussion

4.1. Australia-Wide Dependence Between Extreme Rainfall and Storm Surge

Australia-wide dependence between extreme rainfall and storm surge is plotted in Figure 4 using observed surge data (left plot) and ROMS modeled surge (right plot). The dependence value for each location was estimated as the average of the dependence values calculated for all rain stations within a 100 km radius of the surge location. The maps show that overall there is a good agreement between the dependence estimated using ROMS modeled surge and that estimated using observed surge. The dependence between extreme surge and rainfall is relatively strong ($\alpha \leq 0.9$) to moderate ($\alpha \leq 0.99$) along the majority of Australian coastline. The dependence is statistically significant at 68 out of the 79 tide gauges (established using a bootstrap method, Efron & Tibshirani, 1994).

For both observed and ROMS surge data sets, the dependence is strongest in the north and northwest of Australia, followed by the west and northeast of Australia. In contrast, the dependence is weak and/or statistically insignificant ($\alpha > 0.99$) along southeast coast of Western Australia, along small parts of the South Australian coastline, and along the eastern part of the Victorian coast near Bass Strait. These results are also consistent with those shown in Figure 4a (Zheng et al., 2013). One interesting finding relates to the weak dependence estimate from observations at the northern tip of Queensland (Figure 4a shows an estimate of

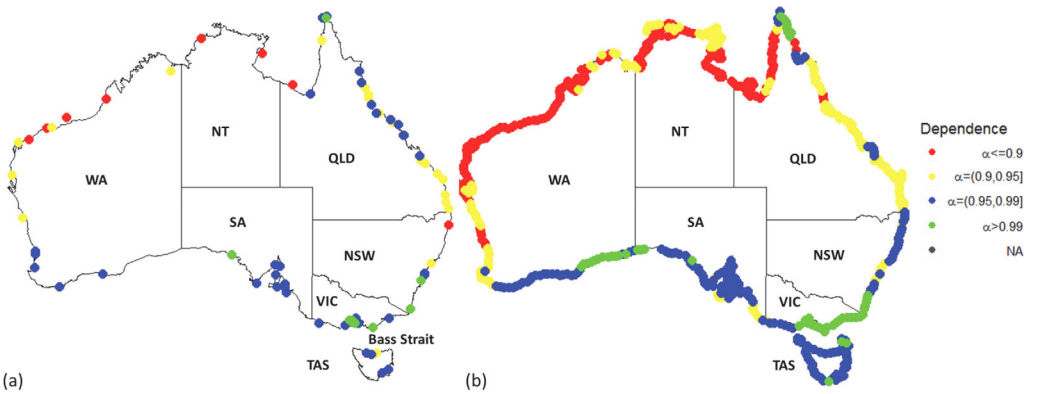

Figure 4. Australian wide dependence mapping between extreme rainfall and storm surge using (a) observed surge and (b) ROMS modeled surge. (*Note.* An alpha value of unity indicates complete independence and an alpha value of less than 0.9 indicates relatively strong dependence in the Australian context.)

0.99). The modeled dependence in Figure 4b concurs with this observation and also shows a region of stronger dependence in locations immediately south of this location, highlighting the benefits of using ROMS in data-sparse regions. Possible explanations for the weak dependence in this region include: (1) reduced tropical cyclone activity in this region compared to the other parts of north and northeast of Australia (Lavender et al., 2015); (2) the potential for an abrupt change of tidal regime due to changed bathymetry; and (3) greater variability of the dependence estimates due to a limited number of rain gauges in this region.

Interpreting the results in the context of flood risk, it should be noted that although the results in Figure 4 are based on surge, the flood risk will depend on the total ocean water level. In regions where storm surge dominates the overall sea level, the dependence between sea level and rainfall is likely to follow a similar pattern to that indicated in Figure 4. In contrast, in regions where astronomical tide is the dominating process, the dependence between extreme sea level and rainfall events is likely to be weaker than presented in Figure 4. This latter case is likely to be particularly relevant in northern Australia where the tidal range can be extremely high.

4.2. Meteorological Drivers of Different Extreme Conditions

To provide insight into the physical drivers of extreme conditions influencing the dependence between extreme storm surge and rainfall, we examined the synoptic weather systems most frequently influencing rain-only, surge-only, and the coincident extreme events at a sample of six locations representing different climate regions along the Australian coastline: Broome, Fremantle, Adelaide, Cape Ferguson, Sydney, and Hobart (for locations see Figure 2). The synoptic typing results are in the form of composite pressure maps, obtained using methods described in section 3.2. A summary of the synoptic typing results is shown in Figure 5.

Starting with Broome in the tropical northwest, it can be seen that extreme rain-only events are associated with large depressions situated along the coast. The surge-only events are broadly similar to the rain-only events, although they tend to feature a smaller-scale closed low at the coast due to a tropical depression or cyclone that would produce strong onshore winds and lower pressures at Broome. The coincident rainfall and surge events are due to tropical cyclones at coastal locations at or to the south of Broome where onshore winds are generally the strongest.

At Fremantle, the majority (73%) of extreme rainfall events are due to midlatitude frontal systems that produce southwesterly winds along the coast, while a smaller number (15%) of events are of tropical origin. For storm surge-only events, the majority of surges (70%) are associated with large extratropical lows (ETLs) to the southwest of the continent or the associated frontal trough (8%), whereas about 8% are associated with a depression of tropical origin. The majority of coincident events are due to ETLs to the southwest of the state.

For locations along the south coast from Albany to Lorne, the predominant type of weather system causing extreme rainfall and storm surges is a cold frontal system with an associated ETL pressure system. These systems consist of a cold front that typically travels from southwest to northeast along the south coast (see Figure 5 for Adelaide), and accounts for about 50% of the extreme rainfall events and over 86% and 83% of the storm surge and coincident events along the southern coastline based on the first key map type. In the case of the coincident rainfall and surge events, a deeper low and tighter gradient to the north-west of the low are evident, which would tend to be associated with stronger southwesterly winds in the postfrontal flow directed towards the coast. The second synoptic map for the rain-only events in Adelaide, comprising 17% of maps, consists of a depression situated inland to the northeast. Such a weather pattern would not be conducive to storm surges since the coastal wind direction would be westward. The third most prevalent map for rain-only events resembles west-southwesterly flow associated with an ETL, but not as far east as the first synoptic type. For storm surge-only events, the second most prevalent weather type is a trough of low pressure over Adelaide with a closed low pressure system to the immediate southwest of Adelaide, while the third map type represents a frontal system moving into the Tasman with the trough lying from the northwest to southeast and extending across Adelaide.

For Hobart, extreme rain events are caused by frontal movement associated with ETLs to the south in 51% of the cases or by Tasman Sea low pressure systems in 34% of the cases. However, the majority of surge-only (94%) and coincident (88%) events are associated with ETLs, with the low situated to the southeast of Hobart.

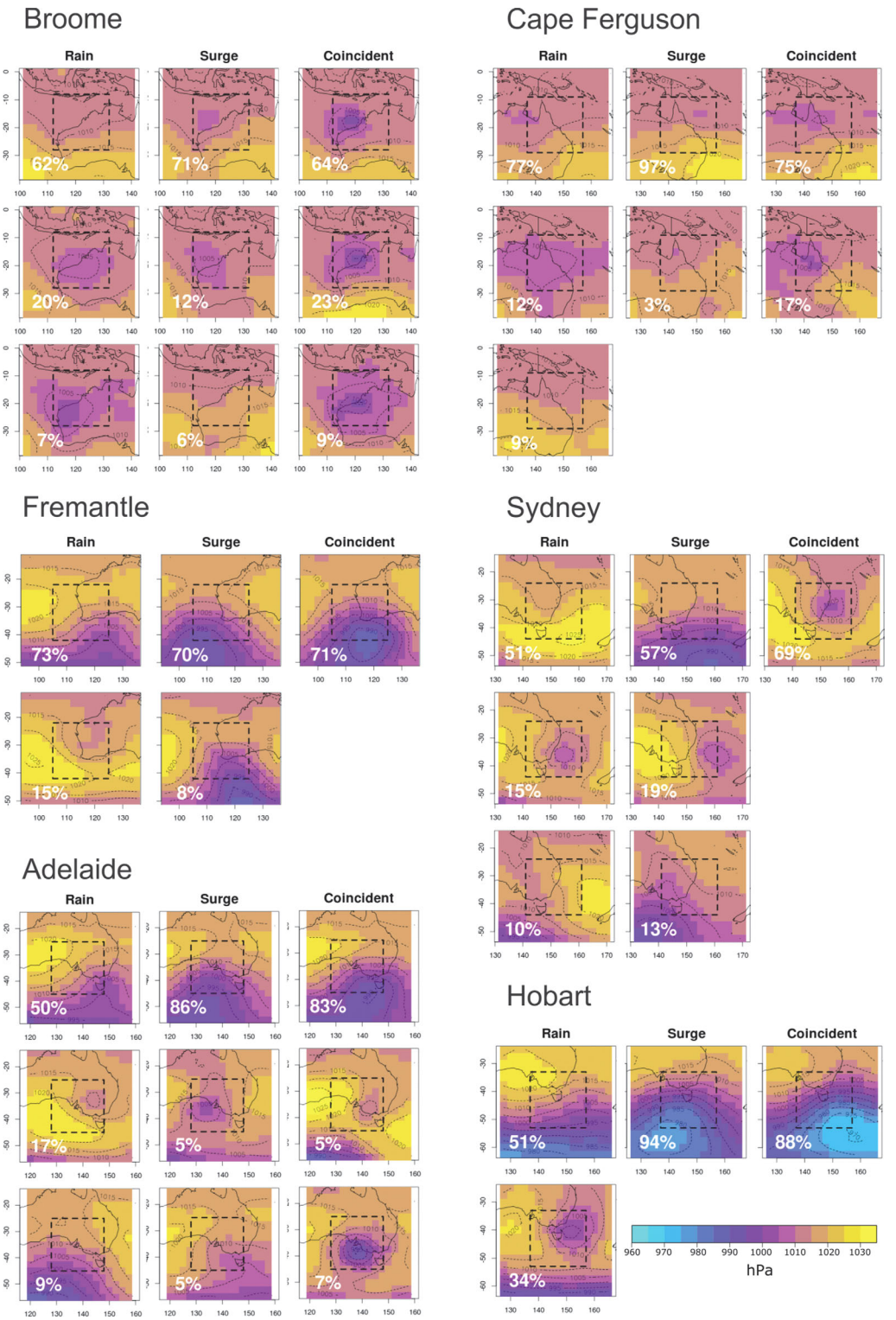

Figure 5. Composite synoptic maps for rain-only, surge-only, and coincident extreme events for six selected locations in Australia. The percentage of maps from each of the rain-only, surge-only, or coincident that contributed to the composite map is indicated. The dashed rectangle indicates the area over which the correlations were calculated.

For Sydney, easterly troughs account for the majority (51%) of extreme rainfall events, while east coast lows account for 15% and frontal trough systems account for 10% of the events. For storm surges, frontal systems cause the majority (57%) of storm surge events while the second most prevalent weather type is

cutoff lows (19%) and the third most prevalent weather type was also a frontal system with a frontal trough extending to the north across the continent. For coincident events, the most frequent pattern was found to be cutoff lows (69%).

Finally, at Cape Ferguson on the tropical northeast coast, extreme rainfall is most commonly associated with patterns that occur during the northeast monsoon, i.e., a pressure trough over inland Australia (77%) with associated warm, moist onshore flow, a depression over much of northern Australia (13%), and a pressure trough with an easterly dip at the coast (9%). For storm surges, all of the events are due to a tropical cyclone in the Tasman Sea (97%) or at the coast (3%) (note that compositing of the maps reduces the definition of the cyclones) while the coincident events occur during or shortly after a cyclone makes landfall.

4.3. Seasonal Variation in Dependence Between Extreme Rainfall and Storm Surge

To further compare between the dependence estimated using modeled and observed surge, the seasonal variability of the dependence along the Australian coastline and its potential meteorological causes were examined. The dependence maps for each season across Australia produced using the observed and ROMS surge are provided in Figure 6. Seasons are defined as spring (September, October, and November), summer (December, January, and February), autumn (March, April, and May), and winter (June, July, and August).

There are significant seasonal differences in the dependence between extreme storm surge and rainfall along the north and northwest coast of Australia, where dependence is very strong in summer and autumn, and becomes insignificant in spring and winter. This distinct difference between the warmer and cooler times of the year is mainly related to tropical cyclone activity: the majority of storm surge-related extreme events in this region are associated with tropical cyclones and tropical lows, which are frequent during the warmer months and can cause extremely high surge and heavy rainfall (Haigh et al., 2014a). During the cooler months, there are fewer surge events in this region, and they often have much smaller magnitudes, which do not exceed the threshold value of surge (i.e., the gray dots in Figure 6).

Along the south coast of Australia, seasonality in dependence is only evident at a few locations. At Esperance on the south coast of Western Australia, the dependence is strong in summer, relatively strong in autumn and becomes insignificant during the rest of the year. Although not common, coincident extreme storm surge and rainfall in this region are likely to be associated with low pressure systems to the northwest

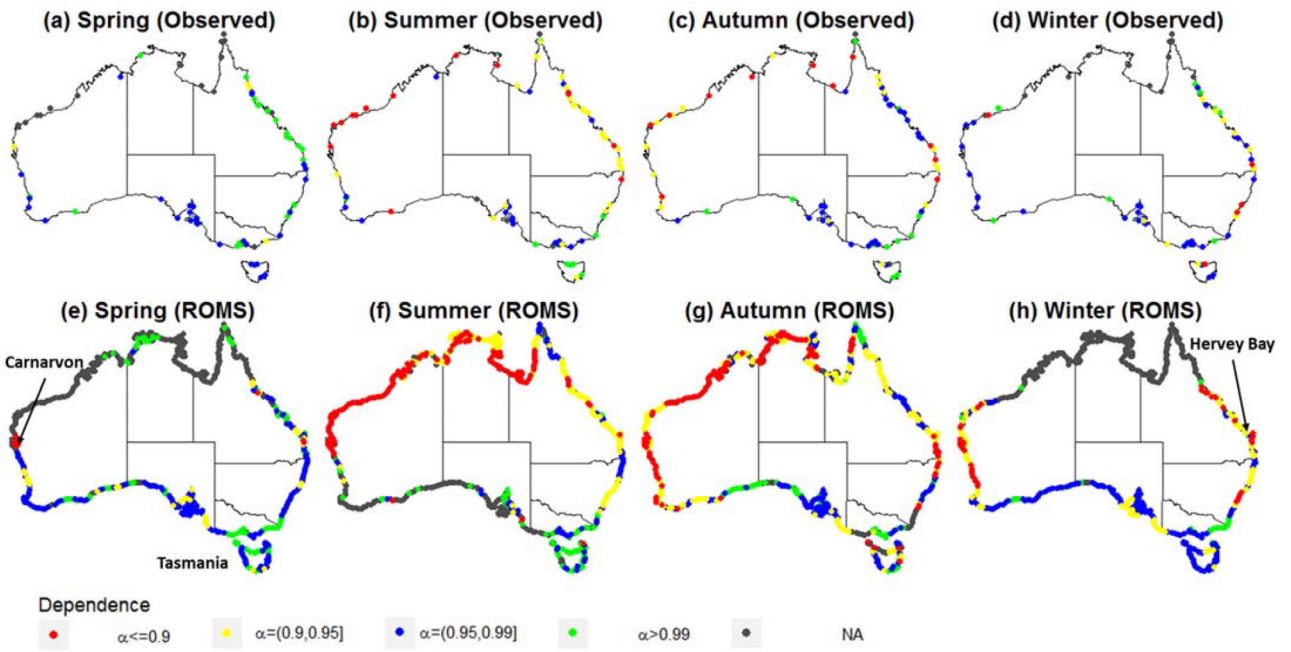

Figure 6. (plots a–d) Seasonal dependence mapping between extreme rainfall and storm surge along Australian coastline using observed surge and (plots e–h) ROMS modeled surge. Gray dots indicate locations where the dependence parameter cannot be estimated due to a lack of data (e.g., no overlapping rainfall and surge data, no rainfall gauge within 100 km of surge locations or no data available above the threshold values).

of the continent and a ridge of high pressure to the southwest (see Figure 5 for Fremantle). Along the northern coast of Tasmania near Bass Strait, there is increased dependence in winter, as in this region, most coincident extreme storm surge and heavy rainfall events are caused by a frontal trough (see Figure 5 for Hobart). This east-traveling cold frontal system often occurs in winter and brings both strong wind and heavy rainfall.

Along the east coast of Australia, seasonal variability in dependence is more evident than along the south. Along the northeast Australian coast (especially in central Queensland), the dependence is weak in spring, strong in summer, slightly reduced in autumn, and relatively strong again in winter. The dependence between extreme storm surge and rainfall in this region is dominated by tropical cyclones in summer, and is influenced by east coast lows during other seasons (see Figure 5 for Cape Ferguson). East coast lows are most frequent in winter (Abbs & McInnes, 2010; McInnes & Hubbert, 2001), which explains the increased dependence in this region in winter. In the southeast of the Australian coast (especially in central New South Wales), the dependence in summer and autumn is reduced compared to the northeast region. This is because the impact of tropical cyclones is diminishing in this region compared to the more northern parts of the coastline, so that the dependence between extreme storm surge and rainfall is dominated by low pressure systems (see Figure 5 for Sydney), which can occur at any time of the year. Again, the more significant and frequent east coast lows in winter (Abbs & McInnes, 2010; McInnes & Hubbert, 2001) contribute to the increased dependence along the New South Wales coast during this season.

Two locations that show anomalous results compared to the surrounding regions in terms of seasonal variability of dependence are Hervey Bay near the eastern tip of Australia and Carnarvon near the western tip of the Australian coast. The dependence at Hervey Bay in winter is insignificant, whereas the dependence at several nearby locations for the same season is very strong (Figure 6h). Furthermore, there is some inconsistency near Carnarvon in the seasonality of dependence estimated using observed and modeled surge. Therefore, Hervey Bay and Carnarvon are selected for further analysis below.

4.4. Hervey Bay in Queensland and Carnarvon in Western Australia

Hervey Bay is located in Queensland on the east coast of Australia (Figure 7a) and represents a transitional area where the impact of tropical cyclones from the north is reducing and the impact of easterly low pressure systems from the south is increasing. Considering the good agreement between observed and modeled surge along the majority of the east coast of Australia, local bathymetry is the most likely cause of the significant drop in dependence within Hervey Bay in winter compared to nearby locations on the western side of Fraser Island (see Figure 7b). Hervey Bay is north-facing and sheltered from easterly wind by Fraser Island. During the warmer months of the year, the geometry of Hervey Bay provides little protection against tropical cyclones largely coming from the north, which results in similar dependence at Hervey Bay compared to nearby locations. However, in winter most storm surge events are associated with low pressure systems to the east. Fraser Island provides high levels of protection against the easterly winds caused by

Figure 7. (a) Locations of Hervey Bay in Queensland and Carnarvon in Western Australia and (b) the winter dependence map around Hervey Bay estimated using ROMS modeled surge data.

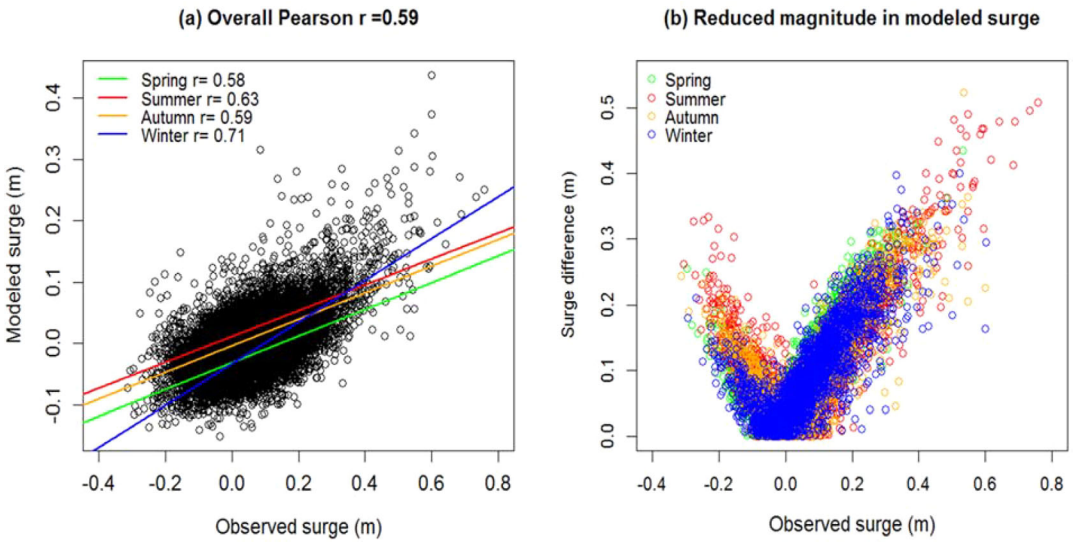

Figure 8. Comparison of ROMS modeled and observed storm surge at Carnarvon in Western Australia. Plot (a) shows the Pearson correlation between the modeled and observed storm surge is 0.59, which is lower than the average value of 0.7 along the Australian coastline. The colored lines show the fitted linear relationship between observed and modeled surge in each season. Plot (b) shows the absolute difference between the modeled and observed storm surge in each season, which increases with the magnitude of observed surge.

these systems, which significantly reduces the magnitude of storm surge. Thus, the dependence between extreme surge and rainfall is also reduced.

The second location for detailed review is Carnarvon, which is located about 900 km north of Fremantle near the western tip of Australia, as shown in Figure 7a. It is also a transitional location where extreme surge is associated with tropical cyclones and tropical lows in the warmer months of the year and frontal systems in the cooler months of the year. To investigate the reduced seasonality in dependence from ROMS at Carnarvon, the observed and modeled surge, as well as their difference, are plotted in Figure 8. From Figure 8a, the Pearson correlation between the observed and modeled surge at Carnarvon is 0.59, which is somewhat lower than the average value of 0.7 along the Australian coastline. In addition, the range of ROMS surge (i.e., −0.2 to 0.4 m) is significantly smaller than observed (i.e., −0.4 to 0.8 m), and the absolute difference between the modeled and observed surge increases with the magnitude of surge (Figure 8b).

The systematic difference between the observed and ROMS modeled storm surge at Carnarvon is likely to be caused by a combination of the local bathymetry, the resolution of ROMS and its meteorological inputs. ROMS has a 5 km resolution; but, this may not be sufficient at locations where bathymetry is complex and shallow, such as near Carnarvon. ROMS performs relatively poorly at locations where a large tidal signal propagates over a fairly shallow shelf. In addition, the coarse meteorological forcing taken from the CFSR reanalysis data only weakly includes the effects of tropical cyclones, which can have a significant impact on modeled storm surge in tropical cyclone affected regions (Haigh et al., 2014b; Muis et al., 2016). This explains the better performance of ROMS in winter at Carnarvon (shown in Figure 8a), as most of tropical cyclones occur between December and April. This effect is also confirmed by the fact that ROMS modeled storm surge generally has smaller magnitude compared to observations along the north, northwest and northeast coast of Australia affected by tropical cyclones. In addition, this systematic difference could also be contributed by the fact that ROMS modeled surge was forced by the meteorological forcing only and therefore the tide-surge interaction is not considered. However, this is unlikely to have a significant impact on the resulting dependence value, which is mainly determined by the ranking order of the bivariate data set of surge and rainfall.

The weak effect of tropical cyclones modeled in ROMS is considered to be the major cause of reduced seasonality in dependence estimated using the model in this transitional region. When the magnitude of extreme surge caused by tropical cyclones in the warmer seasons is reduced more than those caused by frontal systems in the cooler seasons, the difference between extreme surges in these two periods is

reduced. This in turn results in a reduction in seasonal variation in dependence between extreme surge and rainfall, and explains the increased modeled dependence along the west coast of Australia shown in Figure 6h. Interestingly, although this effect is likely to explain the results for Carnarvon, the weak effect of tropical cyclones in ROMS has not had a significant impact on the seasonal dependence in the north of Australia. This is because in northern Australia, tropical cyclones are likely to be the only major cause of large storm surges over the 99th percentile threshold (Wu et al., 2017). Therefore, the reduced effect of tropical cyclones will not change the ranking of major surge events, and thus would have less influence on the dependence value.

Other potential contributors to the discrepancies in seasonal variability of dependence estimated using observed and modeled surge along the western coast of Australia include the relatively large steric component of sea levels in this region (McInnes et al., 2016) and extreme sea level high-frequency oscillations due to infragravity waves or meteotsunamis (Pattiaratchi & Wijeratne, 2014). Both effects are not modeled in barotropic models, such as ROMS (Haigh et al., 2014b); however, they are present in observed surge data (McInnes et al., 2016; Pattiaratchi & Wijeratne, 2014). In addition, the location of a tide gauge may also have some impact on the dependence analysis. It was found in a previous study that the dependence between storm surge and rainfall estimated using observed nontidal residual is likely to be higher at the mouths of major rivers, as the storm surge record may be influenced by river inflows as well as oceanic processes (Zheng et al., 2014); whereas riverine floods are not modeled in ROMS. However, this impact is likely to be minimal and extreme surge and rainfall are dependent regardless of the location of the tide gauge being near or far away from the river mouth (Zheng et al., 2014).

5. Summary and Conclusions

This study extends previous research by estimating the dependence between extreme storm surge and rainfall along the Australian coastline using reanalysis data from a hydrodynamic model—the Regional Ocean Modeling System (ROMS)—and examining the possible meteorological forcing behind different extreme conditions. ROMS provides surge data at 5 km spatial resolution across the entire Australian coastline, which allows an updated dependence map for Australia at much finer scale. Our results show that dependence estimated using reanalysis data generally matches that estimated using observed data across Australia, but with the ROMS data also providing valuable insights into dependence in regions that lack sufficiently long observational records. The dependence between extreme storm surge and rainfall is generally strongest in the north and northwest of Australia, followed by the northeast coast. The dependence is generally weak along the south coast and Tasmania, and is insignificant along the south-east coast near Victoria and south New South Wales.

The meteorological forcing behind each of the different extreme conditions—namely rain-only, surge-only, and coincident extremes—was investigated at six locations representing different climate regions of the Australian coast. Our results show that along the northwest coast of Australia, both types of single-driver extreme events are caused by large depressions along the coast; whereas the coincident extremes are most likely due to tropical cyclones. Along the south coast of Australia, including the south-west, most extreme rainfall events are caused by cold frontal systems, whereas surge-related extremes (e.g., surge-only and coincident extremes) are associated with large extratropical lows. Similar patterns can be found in southeast Australia near Hobart, except that the extratropical lows are situated to the southeast of the affected region. Along the east coast of Australia, extreme rainfall events are mostly related to pressure troughs, while surge-related extremes are often associated with tropical cyclones in the northeast, or frontal systems or cutoff lows in the south east.

The seasonality of dependence between extreme storm surge and rainfall across Australia is also investigated. Our results show that there is strong seasonal variation in dependence along the north and northwest of Australian coast, followed by the northeast, where extreme storm surges are dominated by tropical cyclones in summer and autumn. Along the south coast of Australia, seasonality in dependence is most evident along the south-east coast near Victoria and Tasmania, where extreme storm surge events often coincide with heavy rainfall in winter due to frequent east-traveling frontal systems. Seasonal variation in dependence estimated using reanalysis surge data is less consistent with that estimated using observed data. This is particularly the case at locations where extreme surges are driven by different processes during

different times of the year, and one or more of these processes are not well represented in the hydrodynamic model (e.g., tropical cyclones). It should be noted that although the spatial and seasonal variation in dependence strength caused by seasonal variation in weather patterns is often location-specific, the methodology presented in this study can be used to examine the dependence strength between extreme rainfall and storm surge anywhere around the world.

This study confirms that reanalysis data from hydrodynamic models can be used to estimate the dependence between extreme surge and rainfall with a reasonable level of confidence where observed data are not available. This allows for assessment of future flood risk under changing meteorological conditions, for example due to climate change. However, special care should be given to locations where the model is not performing well due to complex bathymetry, the coarse resolution of the model, the model's boundary conditions, or for cases where one of the mechanisms (e.g., tropical cyclones) is not well represented in the model. In these cases, deep understanding of the meteorological forcing behind different extreme conditions can improve the confidence in the dependence estimated using modeled data. This understanding can also provide better support to applications, such as flood forecasting and flood warning system development, which rely on meteorological inputs.

Acknowledgments
We would like to thank Australian Research Council and Western Australian Water Corporation for funding under Linkage Project LP150100359. We thank the Bureau of Meteorology (http://www.bom.gov.au/) for providing the observed data used in this study. We also wish to thank Deborah Abbs for valuable discussions and assistance in relation to the synoptic typing. Kathleen McInnes, Julian O'Grady, and Ron Hoeke's contribution is supported by the Earth System and Climate Change Hub of Australian Government's National Environmental Science Programme. The observed data used in this study are available from the Bureau of Meteorology (http://www.bom.gov.au/) and are restricted for research purposes only. The modeled data used are available from CSIRO at the following online repository (https://data.csiro.au/dap/landingpage?execution=e1s2&_eventId=viewDescription). The authors would also like to thank the two anonymous reviewers, whose comments and suggestions have improved the paper.

References

Abbs, D., & McInnes, K. (2010). *Coincident extreme rainfall and storm surge events in southern Australia* (report EP182375). Aspendale, Vic: Centre for Australian Weather and Climate Research, CSIRO Marine and Atmospheric Research.

Acreman, M. C. (1994). Assessing the joint probability of fluvial and tidal floods in the river roding. *Water and Environment Journal*, *8*(5), 490–496. https://doi.org/10.1111/j.1747-6593.1994.tb01140.x

Australian Bureau of Statistics (2004). *1301.0—Year Book Australia*. Canberra, ACT: Australian Bureau of Statistics.

Bevacqua, E., Maraun, D., Hobæk Haff, I., Widmann, M., & Vrac, M. (2017). Multivariate statistical modelling of compound events via pair-copula constructions: Analysis of floods in Ravenna (Italy). *Hydrology and Earth System Sciences*, *21*(6), 2701–2723. https://doi.org/10.5194/hess-21-2701-2017

Casagrande, L., Tomasella, J., dos Santos Alvalá, R. C., Bottino, M. J., & de Oliveira Caram, R. (2017). Early flood warning in the Itajaí-Açu River basin using numerical weather forecasting and hydrological modeling. *Natural Hazards*, *88*(2), 741–757. https://doi.org/10.1007/s11069-017-2889-0

Colberg, F., & McInnes, K. L. (2012). The impact of future changes in weather patterns on extreme sea levels over southern Australia. *Journal of Geophysical Research: Oceans*, *117*, C08001. https://doi.org/10.1029/2012JC007919

Coles, S. (2001). *An introduction to statistical modeling of extreme values*. London, UK: Springer.

Coles, S., Heffernan, J., & Tawn, J. (1999). Dependence measures for extreme value analyses, *Extremes*, *2*(4), 339–365. https://doi.org/10.1023/a:1009963131610

Efron, B., & Tibshirani, R. J. (1994). *An Introduction to the Bootstrap*. New York, NY: Chapman and Hall.

Haigh, I. D., MacPherson, L. R., Mason, M. S., Wijeratne, E. M. S., Pattiaratchi, C. B., Crompton, R. P., et al. (2014a). Estimating present day extreme water level exceedance probabilities around the coastline of Australia: tropical cyclone-induced storm surges. *Climate Dynamics*, *42*(1), 139–157. https://doi.org/10.1007/s00382-012-1653-0

Haigh, I. D., Wijeratne, E. M. S., MacPherson, L. R., Pattiaratchi, C. B., Mason, M. S., Crompton, R. P., et al. (2014b). Estimating present day extreme water level exceedance probabilities around the coastline of Australia: Tides, extra-tropical storm surges and mean sea level. *Climate Dynamics*, *42*(1), 121–138. https://doi.org/10.1007/s00382-012-1652-1

Hashino, M. (1985). Formulation of the joint return period of two hydrologic variates associated with a Poisson process. *Journal of Hydroscience and Hydraulic Engineering*, *3*(2), 73–84.

Hawkes, P. J. (2008). Joint probability analysis for estimation of extremes. *Journal of Hydraulic Research*, *46*(Suppl. 2), 246–256. https://doi.org/10.1080/00221686.2008.9521958

Hopley, D. (1974). The cyclone Althea storm surge. *Australian Geographical Studies*, *12*(1), 90–106. https://doi.org/10.1111/j.1467-8470.1974.tb00304.x.

Hunt, H. A. (1914). *Results of rainfall observations made in Queensland: including all available annual rainfall totals from 1040 stations for all years of record up to 1913, together with maps and diagrams*. Melbourne, Vic: Commonwealth Bureau of Meteorology.

Intergovernmental Panel on Climate Change (2012). Managing the risks of extreme events and disasters to advance climate change adaptation. In C. B. Field et al. (Eds.), *A special report of working groups I and II of the intergovernmental panel on climate change* (582 p.). New York, NY: Intergovernmental Panel on Climate Change.

Kalnay, E., Kanamitsu, M., Kistler, R., Collins, W., Deaven, D., Gandin, L., et al. (1996). The NCEP/NCAR 40-Year Reanalysis Project. *Bulletin of the American Meteorological Society*, *77*(3), 437–471. https://doi.org/10.1175/1520-0477(1996)077<0437:TNYRP>2.0.CO;2.

Lambert, M., & Kuczera, G. (1996). Approximate joint probability analysis of extreme water levels in coastal catchments. In *Stochastic hydraulics. Proc. symposium*, Mackay, Australia (pp. 251–258).

Lavender, S., Tory, K., Ye, H., & Rafter, T. (2015). *Refining Australian region tropical cyclone projections*. Hobart, Australia: GREENHOUSE, Collaboration for Australian Weather and Climate Research (CAWCR).

Ledford, A. W., & Tawn, J. A. (1997). Modelling dependence within joint tail regions. *Journal of the Royal Statistical Society*, *59*(2), 475–499. https://doi.org/10.1111/1467-9868.00080

Leonard, M., Westra, S., Phatak, A., Lambert, M., van den Hurk, B., McInnes, K., et al. (2014). A compound event framework for understanding extreme impacts. *Wiley Interdisciplinary Reviews*, *5*(1), 113–128. https://doi.org/10.1002/wcc.252

Lian, J. J., Xu, K., & Ma, C. (2013). Joint impact of rainfall and tidal level on flood risk in a coastal city with a complex river network: A case study of Fuzhou City, China. *Hydrology and Earth System Sciences*, *17*(2), 679–689. https://doi.org/10.5194/hess-17-679-2013

Loganathan, G. V., Kuo, C. Y., & Yannaccone, J. (1987). Joint probability distribution of streamflows and tides in estuaries, (Rappahannock River, USA). *Nordic Hydrology*, *18*(4–5), 237–246.

McInnes, K. L., & Hubbert, G. D. (2001). The impact of eastern Australian cut-off lows on coastal sea levels. *Meteorological Applications*, *8*(2), 229–243. https://doi.org/10.1017/S1350482701002110

McInnes, K. L., Hubbert, G. D., Abbs, D. J., & Oliver, S. E. (2002). A numerical modelling study of coastal flooding. *Meteorology and Atmospheric Physics*, *80*(1), 217–233. https://doi.org/10.1007/s007030200027

McInnes, K. L., White, C. J., Haigh, I. D., Hemer, M., Hoeke, R. A., Holbrook, N. J., et al. (2016). Natural hazards in Australia: Sea level and coastal extremes. *Climatic Change*, *139*(1), 69–83. https://doi.org/10.1007/s10584-016-1647-8

Muis, S., Verlaan, M., Winsemius, H. C., Aerts, J. C. J. H., & Ward, P. J. (2016). A global reanalysis of storm surges and extreme sea levels. *Nature Communications*, *7*, 11969. https://doi.org/10.1038/ncomms11969

Pathiraja, S., Westra, S., & Sharma, A. (2012). Why continuous simulation? The role of antecedent moisture in design flood estimation. *Water Resources Research*, *48*, W06534. https://doi.org/10.1029/2011WR010997

Pattiaratchi, C., & Wijeratne, E. M. S. (2014). Observations of meteorological tsunamis along the south-west Australian coast. *Natural Hazards*, *74*(1), 281–303. https://doi.org/10.1007/s11069-014-1263-8

Permanent Committee on Tides and Mean Sea Level (2007). *The Australian tides manual* (report, Version 4.4, 40 p.). Canberra, Australia: Intergovernmental Committee on Surveying and Mapping (ICSM).

Pugh, D. T. (1987). *Tides, surges, and mean sea-level*, Chichester, UK: John Wiley & Sons.

Resio, D. T., & Westerink, J. J. (2008). Modeling the physics of storm surges. *Physics Today*, *61*, 33–38.

Saha, S., Moorthi, S., Pan, H.-L., Wu, X., Wang, J., Nadiga, S., et al. (2010). The NCEP climate forecast system reanalysis. *Bulletin of the American Meteorological Society*, *91*(8), 1015–1057. https://doi.org/10.1175/2010bams3001.1

Shchepetkin, A. F., & McWilliams, J. C. (2005). The regional oceanic modeling system (ROMS): A split-explicit, free-surface, topography-following-coordinate oceanic model. *Ocean Modelling*, *9*(4), 347–404.

Svensson, C., & Jones, D. A. (2002). Dependence between extreme sea surge, river flow and precipitation in eastern Britain. *International Journal of Climatology*, *22*(10), 1149–1168. https://doi.org/10.1002/joc.794

Svensson, C., & Jones, D. A. (2004). Dependence between sea surge, river flow and precipitation in south and west Britain. *Hydrology and Earth System Sciences*, *8*(5), 973–992. https://doi.org/10.5194/hess-8-973-2004

Tawn, J. A. (1988). Bivariate extreme value theory: Models and estimation. *Biometrika*, *75*(3), 397–415. https://doi.org/10.1093/biomet/75.3.397

Van den Hurk, B., van Meijgaard, E., deValk, P., van Heeringen, K.-J., & Goijer, J. (2015). Analysis of a compounding surge and precipitation event in the Netherlands. *Environmental Research Letters*, *10*, 035001. https://doi.org/10.1088/1748-9326/10/3/035001

Wahl, T., Jain, S., Bender, J., Meyers, S. D., & Luther, M. E. (2015). Increasing risk of compound flooding from storm surge and rainfall for major US cities. *Nature Climate Change*, *5*(12), 1093–1097. https://doi.org/10.1038/nclimate2736. Retrieved from http://www.nature.com/nclimate/journal/v5/n12/abs/nclimate2736.html#supplementary-information

Westra, S. (2012). *Australian rainfall & runoff revision project 18: Interaction of coastal processes and severe weather events—Stage 2 report* (report P18/S2/010). Sydney, NSW: Engineers Australia.

Wu, W., Westra, S., & Leonard, M. (2017). A basis function approach for exploring the seasonal and spatial features of storm surge events. *Geophysical Research Letters*, *44*, 7356–7365. https://doi.org/10.1002/2017GL074357

Yarnal, B. (1993). *Synoptic climatology in environmental analysis*. London, UK: Belhaven Press.

Zheng, F., Westra, S., & Sisson, S. A. (2013). Quantifying the dependence between extreme rainfall and storm surge in the coastal zone. *Journal of Hydrology*, *505*, 172–187. https://doi.org/10.1016/j.jhydrol.2013.09.054

Zheng, F., Westra, S., & Leonard, M. (2014). *Australian rainfall & runoff revision project 18: Coincidence of fluvial flooding events and coastal water levels in estuarine areas—Stage 3 report* (report P18/S3/011). Sydney, NSW: Engineers Australia.